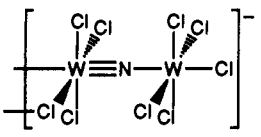

III

geometry are observed at the triply-bonded tungsten atom (W(1) in Figure 5), with the cis chlorides bent away from the nitride ligand and an elongated trans bridging chloride to tungsten distance (W(1)–Cl(1) in Figure 5).

On the basis of its formula, $[W_2(N)Cl_9]^-$ (III) is a d^1 species, formally containing tungsten(VI) and tungsten(V) centers. The solid-state structure, d-electron count, and charge suggest that this species is best described as an adduct in which an anionic tungsten(VI) nitride, $[W(N)Cl_4]^-$, is coordinated via a bridging nitrido ligand to a neutral tungsten(V) chloride fragment, WCl_5. An analogous formulation has previously been reported for the closely related mixed-valence nitride-bridged molybdenum compound $[Mo_2(N)Cl_9]_2[PPh_4]_2$.[29] Structural characterization of this species has shown that it contains a dichloro-bridged dimer of a nitride-bridged dimolybdenum anion analogous to III, and synthetic studies indicate that it can be prepared in excellent yield from the reaction of $[MoNCl_4][PPh_4]$ with $MoCl_5$.[29] In contrast, it is not clear why **10** forms in such good yield in reaction 11 nor is it clear how **10** is produced. Reactions of $W(NPR_3)Cl_5$ (**4**) with WCl_6 do not yield **10** or its analogues, ruling out this simple route to such compounds. One other mixed-valence tungsten(V/VI) dimetallonitride, $[W_2(N)Cl_{10}][AsPh_4]_2$, is known.[30] As for **10**, the details involved in its high-yield synthesis (by decomposition of $[WNCl_4][AsPh_4]$) are not understood.

(29) Godemeyer, T.; Weller, F.; Dehnicke, K. *Z. Anorg. Allg. Chem.* **1987**, *554*, 92-100.
(30) Weller, F.; Liebelt, W.; Dehnicke, K. *Angew. Chem., Int. Ed. Engl.* **1980**, *19*, 220.

Summary and Conclusions

Molybdenum and tungsten phosphoraniminato complexes are readily prepared from the metal(IV) silylimido complexes, $M(NSiMe_3)Cl_2(PMe_3)_3$. Reactions with chlorine produce metal(V) and metal(VI) phosphoraniminato complexes, depending on the number of equivalents of oxidant added, while additions of organophosphine dichlorides yield the metal(IV) phosphoraniminato compounds. The facility of the latter reaction, which can be considered a main-group analogue of the condensation reaction used to form nitrido-bridged metal complexes, suggests that addition of PCl_2R_3 to $L_nM(NSiMe_3)$ may be a useful general route to phosphoraniminato complexes.

Nitrido-bridged complexes, formed either by decomposition of phosphoraniminato species or in attempts to develop alternative syntheses of phosphoraniminato species, have additionally been observed in the molybdenum and tungsten systems described here. These suggest the potential for use of phosphoraniminato complexes as alternative precursors for the synthesis of nitride-bridged transition-metal compounds and materials, an area we are currently exploring.

Acknowledgment. We gratefully acknowledge support of this work by the donors of the Petroleum Research Fund, administered by the American Chemical Society, and by the Air Force Office of Scientific Research, Air Force Systems Command, USAF, Grants Nos. AFOSR-87-0362 and AFOSR-91-0179. We thank Dr. Susan C. Critchlow for assistance with collection of the X-ray diffraction data for **4a**, **7a**·2MeCN, and **10**. N.M.D. thanks the Alfred P. Sloan Research Foundation for a Fellowship (1990-1992).

Supplementary Material Available: Tables of X-ray diffraction data for **4a**, **6a**·toluene, **6b**·2MeCN, **7a**·2MeCN, and **10**, including structure determination summaries, atomic coordinates, interatomic distances, interatomic angles, anisotropic displacement coefficients, and hydrogen atom coordinates and additional ORTEP drawings (42 pages); tables of observed and calculated structure factors (75 pages). Ordering information is given on any current masthead page.

Contribution from the CNR Centro di Studio sulla Sintesi e la Struttura dei Composti dei Metalli di Transizione nei Bassi Stati di Ossidazione, Dipartimento di Chimica Inorganica e Metallorganica dell'Università di Milano, and Istituto di Chimica Strutturistica Inorganica dell'Università di Milano, Via G. Venezian 21, 20133 Milano, Italy

Mixed Rhodium–Osmium Carbonyl Clusters. Synthesis of the Anions $[OsRh_5(CO)_{16}]^-$ and $[OsRh_3(CO)_{12}]^-$ and Crystal Structures of Their (μ-Nitrido)bis(triphenylphosphorus)(1+) Salts

Alessandro Fumagalli,*[1a] Secondo Martinengo,[1b] Gianfranco Ciani,[1c] Massimo Moret,[1c] and Angelo Sironi*[1c]

Received December 2, 1991

The two new anions $[OsRh_5(CO)_{16}]^-$ (**1**) and $[OsRh_3(CO)_{12}]^-$ (**2**) have been obtained, in a 1:1 mixture, by acidification of $[OsRh_4(CO)_{15}]^{2-}$. Alternative synthetic routes have been devised: **1** may be also produced by condensation of Rh^I derivatives on $[OsRh_4(CO)_{15}]^{2-}$ or, more conveniently, with a one-pot synthesis, starting from $Os_3(CO)_{12}$ and $Rh_4(CO)_{12}$; **2** may be obtained by oxidative demolition of $[OsRh_4(CO)_{15}]^{2-}$ with iodine. Both anions were characterized by single-crystal X-ray diffraction of their $[(Ph_3P)_2N]^+$ (PPN) salts. (PPN)$[OsRh_5(CO)_{16}]$: space group $C2/c$, $Z = 8$, $a = 33.665$ (4) Å, $b = 9.752$ (1) Å, $c = 33.785$ (5) Å, $\beta = 94.45$ (1)°, $R = 0.030$, and $R_w = 0.031$ for 5166 independent reflections with $I > 3\sigma(I)$. (PPN)$[OsRh_3(CO)_{12}]$: space group $P2_1/c$, $Z = 4$, $a = 14.707$ (3) Å, $b = 21.371$ (6) Å, $c = 16.095$ (3) Å, $\beta = 102.83$ (2)°, $R = 0.037$, and $R_w = 0.037$ for 3007 independent reflections with $I > 3\sigma(I)$. Anion **1** shows a $Rh_6(CO)_{16}$-like structure with 12 terminal carbonyls (2 on each metal) and 4 triply bridging on the alternate faces of the octahedral skeleton. Anion **2** has a tetrahedral metal frame with an unprecedented ligand disposition, 7 terminal and 5 bridging carbonyls with overall C_s ideal symmetry. ^{13}C NMR spectra in the temperature range 323-183 K evidenced a fluxional behavior in **2**, from complete CO scrambling to a static situation consistent with the solid-state structure; compound **1** was found to be static at room temperature.

Introduction

Our previous investigations on the Os–Rh bimetallic system led to the synthesis and characterization of $[OsRh_4(CO)_{15}]^{2-}$,[2] a product which can be obtained as the $[(Ph_3P)_2N]^+$ (PPN) salt on a several hundred milligrams scale and is therefore a suitable starting material. The study of its reactivity yielded two new species, the anions $[OsRh_5(CO)_{16}]^-$ and $[OsRh_3(CO)_{12}]^-$, here

(1) (a) CNR. (b) Dipartimento di Chimica Inorganica e Metallorganica dell'Università di Milano. (c) Istituto di Chimica Strutturistica Inorganica dell'Università di Milano.

(2) Fumagalli, A.; Garlaschelli, L.; Della Pergola, R. *J. Organomet. Chem.* **1989**, *362*, 197.

0020-1669/92/1331-2900$03.00/0

reported. It must be noted that the former one completes the isostructural triad $[MRh_5(CO)_{16}]^-$ (M = Fe,[3] Ru,[4] Os) allowing an interesting comparison of the relative reactivities, of the structural aspects, and of the ^{13}C NMR chemical shifts.

Results

1. Synthesis of the Anions $[OsRh_5(CO)_{16}]^-$ and $[OsRh_3(CO)_{12}]^-$. The dianion $[OsRh_4(CO)_{15}]^{2-}$,[2] due to its high reduction state, is synthesized and indefinitely stable in strongly reducing conditions such as in markedly basic media under a CO atmosphere; it is thus expected to be reactive toward electrophiles. In fact it was found to be reactive toward acids but giving, instead of the expected corresponding hydride(s), a complex reaction of both oxidation and metal atom redistribution, with formation of a 1:1 mixture of the two title compounds, according to the stoichiometry in (1). The hydrogen and CO evolution were confirmed by

$$2[OsRh_4(CO)_{15}]^{2-} + 2H^+ \rightarrow [OsRh_3(CO)_{12}]^- + [OsRh_5(CO)_{16}]^- + H_2 + 2CO \quad (1)$$

gas-chromatographic analysis of the gases evolved upon addition of excess H_3PO_4 to $(PPN)_2[OsRh_4(CO)_{15}]$ in THF, under N_2. The reaction takes several days in weakly acid media, such as those obtained by moderate addition of CH_3COOH to the methanolic solutions in which $[OsRh_4(CO)_{15}]^{2-}$ is synthesized, whereas with an excess of a stronger acid is completed in a few minutes. Strict IR monitoring of the reaction course at room temperature gave no evidence of products other than those appearing in eq 1, suggesting that the intermediate species, possibly of hydridic nature, are very labile. Reaction 1 is well reproducible and unaffected by the nature of the solvent and of the countercation or by the presence of carbon monoxide; however, from the preparative point of view it is not convenient, as it gives a mixture of the two anions. Therefore we searched for alternative syntheses, specifically tailored for each species.

$[OsRh_5(CO)_{16}]^-$ can be obtained by the reaction of $[OsRh_4(CO)_{15}]^{2-}$ with $[Rh(CO)_2(MeCN)_2]^+$ or $[Rh(CO)_2Cl]_2$. The two Rh^I derivatives however react differently. In the first case a ready 1:1 redox condensation is observed, according to eq 2. In the

$$[OsRh_4(CO)_{15}]^{2-} + [Rh(CO)_2(MeCN)_2]^+ \rightarrow [OsRh_5(CO)_{16}]^- + CO + 2MeCN \quad (2)$$

second case the reaction pathway is quite different, because the addition of 1 equiv of Rh^I leaves some unreacted $[OsRh_4(CO)_{15}]^{2-}$ due to the side formation of $[Rh(CO)_2Cl_2]^-$, as evidenced by IR spectra. Two equivalents of Rh^I are thus required to complete the reaction, as in eq 3. It must be noted however that reactions 2 and 3 always give, besides $[OsRh_5(CO)_{16}]^-$ as the main product (60–70%), some $[OsRh_3(CO)_{12}]^-$ and another product whose characterization is in progress.

$$[OsRh_4(CO)_{15}]^{2-} + [Rh(CO)_2Cl]_2 \rightarrow [OsRh_5(CO)_{16}]^- + [Rh(CO)_2Cl_2]^- + CO \quad (3)$$

On the basis of reaction 1 and of the possible metal atom redistribution equilibria, we developed a convenient one-pot synthesis of $[OsRh_5(CO)_{16}]^-$. The reduction of a mixture of $Os_3(CO)_{12}$ and $Rh_4(CO)_{12}$, taken in the correct 1:5 Os:Rh atomic ratio, gives $[OsRh_4(CO)_{15}]^{2-}$ with the excess of Rh present as $[Rh_7(CO)_{16}]^{3-}$ and/or $[Rh_6(CO)_{15}]^{2-}$.[5] Upon acidification of this mixture, the system evolves to give, after the rapid reaction 1, a slower recombination process of the excess Rh with $[OsRh_3(CO)_{12}]^-$, yielding eventually pure $[OsRh_5(CO)_{16}]^-$. This reequilibration takes a several day period at room temperature but may be completed in a few hours with moderate heating at 50–60 °C.

Unfortunately, a similar one-pot synthesis is *not* applicable to the preparation of $[OsRh_3(CO)_{12}]^-$. In fact the reduction of a mixture of $Os_3(CO)_{12}$ and $Rh_4(CO)_{12}$, with an Os:Rh atomic ratio of 1:3, yields again $[OsRh_4(CO)_{15}]^{2-}$ but now with an excess of Os present essentially as $[HOs_3(CO)_{11}]^-$.[6] Acidification of this mixture proceeds according to the previous reaction 1, but the $[OsRh_5(CO)_{16}]^-$ which is formed does not undergo the desired metal redistribution with the excess Os to give the mixed-metal tetranuclear anion. Very likely, both the stability of the hexanuclear anion and the low solubility of the Os species formed in the acidic reaction medium hinder the metal atom redistribution.

A more reliable synthesis of $[OsRh_3(CO)_{12}]^-$ has been devised by controlled oxidative demolition of $[OsRh_4(CO)_{15}]^{2-}$; treatment of this anion with I_2 results in the selective detachment of a single Rh atom (eq 4). The reaction however always gives as a by-

$$[OsRh_4(CO)_{15}]^{2-} + I_2 \rightarrow [OsRh_3(CO)_{12}]^- + [Rh(CO)_2I_2]^- + CO \quad (4)$$

product some $[OsRh_5(CO)_{16}]^-$, probably because of a side reaction of condensation similar to (3) between some just formed Rh^I derivative and yet unreacted $[OsRh_4(CO)_{15}]^{2-}$. In any case it has to be said that the tetranuclear cluster slowly decomposes in solution to give some $[OsRh_5(CO)_{16}]^-$ and other unidentified products. Thus, repeated crystallizations by the slow-diffusion technique are not effective to obtain a pure product; the best way is to separate manually the single crystals.

2. Crystal Structure of $(PPN)[OsRh_5(CO)_{16}]$. The crystal structure consists of a packing of $(PPN)^+$ cations and $[OsRh_5(CO)_{16}]^-$ anions in the molar ratio 1:1 with normal van der Waals contacts between the atoms of different ionic fragments. Selected bond distances and angles are listed in Table I. The molecular structure of **1** (see Figure 1) is very similar to the structures of the isoelectronic clusters $[MRh_5(CO)_{16}]$ (M = Fe,[3] Ru[4]) sharing similarly the $[Rh_6(CO)_{16}]$ stereogeometry;[7] each metal atom carries two terminal carbonyl ligands, and four triply bridging COs span alternate faces of the MRh_5 octahedron. The average metal–metal bond distance (2.776 (3) Å) in **1** is longer than that found in the $[MRh_5(CO)_{16}]^-$ anions (2.750 Å for M = Fe, 2.769 Å for M = Ru), and there is a clear cluster expansion along the series of the Fe, Ru, and Os derivatives. All the metal atoms have variable mixed Os/Rh occupancies, and M5 is the metal carrying the major percentage of Os character (45%, on the basis of the refined occupancies). As a matter of fact the M5–M distances are, on average, slightly longer than the remaining M–M inter-

Table I. Selected Bond Distances (Å) and Angles (deg) in $[OsRh_5(CO)_{16}]^-$

M1–M2	2.748 (1)	M2–M4	2.769 (1)	M3–M5	2.787 (1)
M1–M3	2.783 (1)	M2–M5	2.778 (1)	M3–M6	2.781 (1)
M1–M5	2.791 (1)	M2–M6	2.776 (1)	M4–M5	2.783 (1)
M1–M6	2.768 (1)	M3–M4	2.779 (1)	M4–M6	2.772 (1)
M1–C11	1.875 (9)	C11–O11	1.138 (8)	M1–C11–O11	179.0 (8)
M1–C12	1.884 (8)	C12–O12	1.142 (8)	M1–C12–O12	177.7 (7)
M2–C21	1.874 (9)	C21–O21	1.144 (9)	M2–C21–O21	178.3 (8)
M2–C22	1.886 (9)	C22–O22	1.117 (9)	M2–C22–O22	177.3 (8)
M3–C31	1.873 (8)	C31–O31	1.130 (8)	M3–C31–O31	176.4 (8)
M3–C32	1.886 (9)	C32–O32	1.127 (9)	M3–C32–O32	178.8 (8)
M4–C41	1.868 (11)	C41–O41	1.134 (10)	M4–C41–O41	175. (1)
M4–C42	1.894 (8)	C42–O42	1.131 (8)	M4–C42–O42	178.1 (8)
M5–C51	1.888 (10)	C51–O51	1.152 (9)	M5–C51–O51	178.2 (8)
M5–C52	1.891 (9)	C52–O52	1.130 (8)	M5–C52–O52	178.1 (8)
M6–C61	1.886 (8)	C61–O61	1.131 (9)	M6–C61–O61	178.3 (9)
M6–C62	1.892 (9)	C62–O62	1.127 (8)	M6–C62–O62	178.4 (8)
M3–C531	2.308 (8)	C531–O531	1.157 (8)	M1–C531–O531	130.3 (6)
M1–C531	2.250 (8)			M3–C531–O531	131.7 (7)
M5–C531	2.159 (8)			M5–C531–O531	139.6 (7)
M2–C542	2.276 (8)	C542–O542	1.170 (8)	M2–C542–O542	130.8 (7)
M4–C542	2.244 (8)			M4–C542–O542	130.5 (6)
M5–C542	2.140 (8)			M5–C542–O542	139.3 (6)
M1–C621	2.269 (8)	C621–O621	1.144 (8)	M1–C621–O621	134.1 (7)
M2–C621	2.243 (8)			M2–C621–O621	133.3 (6)
M6–C621	2.193 (9)			M6–C621–O621	135.8 (7)
M3–C643	2.229 (8)	C643–O643	1.156 (8)	M3–C643–O643	134.2 (7)
M4–C643	2.258 (8)			M4–C643–O643	133.7 (7)
M6–C643	2.202 (9)			M6–C643–O643	134.1 (7)

(3) (a) Ceriotti, A.; Longoni, G.; Della Pergola, R.; Heaton, B. T.; Smith, D. O. *J. Chem. Soc., Dalton Trans.* **1983**, 1433. (b) Slovokhotov, Y. L.; Struchkov, Y. T.; Lopatin, V. E.; Gubin, S. P. *J. Organomet. Chem.* **1984**, *266*, 139.
(4) Pursianen, J.; Pakkanen, T. A.; Smolander, K. *J. Chem. Soc., Dalton Trans.* **1987**, 781.
(5) Martinengo, S.; Chini, P. *Gazz. Chim. Ital.* **1972**, *102*, 344.
(6) Eady, C. R.; Johnson, B. F. G.; Lewis, J.; Malatesta, M. C. *J. Chem. Soc., Dalton Trans.* **1978**, 1358.
(7) Corey, E. R.; Dahl, L. F.; Beck, W. *J. Am. Chem. Soc.* **1963**, *85*, 1202.

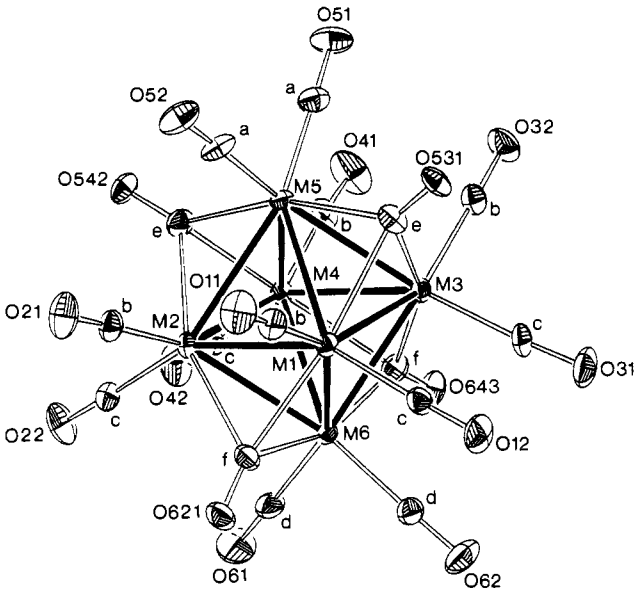

Figure 1. View of the $[OsRh_5(CO)_{16}]^-$ anion. The C atoms of the carbonyl groups bear the same numbering as the respective connected O atoms in the crystal structure. The carbon lettering (a–f) refers to the ^{13}C NMR spectrum, and M5 must be considered to be the Os atom.

Table II. Selected Bond Distances (Å) and Angles (deg) in $[OsRh_3(CO)_{12}]^-$

Os–Rh1	2.878 (1)	Os–Rh3	2.948 (1)	Rh1–Rh3	2.705 (2)
Os–Rh2	2.896 (1)	Rh1–Rh2	2.733 (2)	Rh2–Rh3	2.697 (1)
Os–C1	1.90 (2)	C1–O1	1.14 (2)	Os–C1–O1	178 (1)
Os–C2	1.90 (2)	C2–O2	1.14 (2)	Os–C2–O2	178 (2)
Os–C3	1.90 (2)	C3–O3	1.15 (2)	Os–C3–O3	176 (2)
Rh1–C11	1.88 (2)	C11–O11	1.14 (2)	Rh1–C11–O11	177 (2)
Rh2–C21	1.89 (2)	C21–O21	1.12 (2)	Rh2–C21–O21	179 (2)
Rh3–C31	1.92 (2)	C31–O31	1.13 (2)	Rh3–C31–O31	176 (2)
Rh3–C32	1.85 (2)	C32–O32	1.15 (2)	Rh3–C32–O32	176 (2)
Os–CB1	2.18 (2)	CB1–OB1	1.19 (2)	Os–CB1–OB1	137 (1)
Rh1–CB1	1.97 (2)			Rh1–CB1–OB1	135 (1)
Os–CB2	2.23 (2)	CB2–OB2	1.17 (2)	Os–CB2–OB2	137 (1)
Rh2–CB2	1.97 (2)			Rh2–CB2–OB2	136 (1)
Rh1–CB12	2.09 (2)	CB12–OB12	1.15 (2)	Rh1–CB12–OB12	138 (1)
Rh2–CB12	2.10 (2)			Rh2–CB12–OB12	141 (1)
Rh1–CB13	2.06 (2)	CB13–OB13	1.17 (2)	Rh1–CB13–OB13	146 (1)
Rh3–CB13	2.16 (2)			Rh3–CB13–OB13	134 (1)
Rh2–CB23	2.04 (2)	CB23–OB23	1.18 (2)	Rh2–CB23–OB23	141 (1)
Rh3–CB23	2.12 (2)			Rh3–CB23–OB23	138 (1)

actions (2.785 (3) vs 2.772 (4) Å), while the M5–C_{br} (br = bridging) distances are shorter than the other M–C_{br} distances (2.15 (1) vs 2.25 (1) Å). These perturbations are those expected to occur when the large Os^- fragment substitutes the smaller Rh atom; in fact the M–M interactions are mainly affected by the metal size, while the M–C_{br} bonds are also strongly affected by the need for charge delocalization.

3. Crystal Structure of (PPN)[$OsRh_3(CO)_{12}$]. The crystal structure consists of a packing of $(PPN)^+$ cations and $[OsRh_3(CO)_{12}]^-$ anions in the molar ratio 1:1 with normal van der Waals contacts between atoms of different ionic fragments. An ORTEP plot of the $[OsRh_3(CO)_{12}]^-$ anion is reported in Figure 2 together with the atom-labeling scheme; selected bond distances and angles are listed in Table II. $[OsRh_3(CO)_{12}]^-$ has a tetrahedral metal skeleton surrounded by twelve carbonyl groups, seven terminal and five bridging all but one of the M–M edges. The overall carbonyl stereochemistry, of idealized C_s symmetry, is novel, but it can be obtained from that of $[Rh_4(CO)_{12}]$[8] by bending two (formerly) terminal equatorial COs toward the apical metal atom

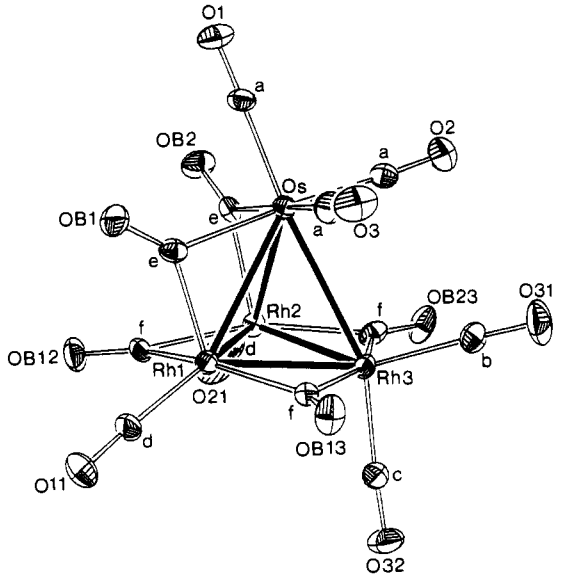

Figure 2. View of the $[OsRh_3(CO)_{12}]^-$ anion. The C atoms of the carbonyl groups bear the same numbering as the respective connected O atoms in the crystal structure. The carbon lettering (a–f) refers to the ^{13}C NMR spectrum. The molecules have C_s symmetry; the idealized mirror plane contains the Os, C1, O1, Rh3, C31, O31, C32, O32, CB12, and OB12 atoms.

and slightly rearranging all the other COs (but maintaining their original connectivity).

All the Rh–Rh bonds are spanned by a bridging CO, and their lengths range from 2.697 (1) to 2.733 (2) Å, with a mean value of 2.712 Å; the three Os–Rh edges, on the contrary, fall in two different classes, being two short (average 2.887 Å) and one long (2.948 (1) Å), according to the presence or absence of a bridging CO. Note, nevertheless, that these Os–Rh interactions are longer than the Os–Os distances in $Os_3(CO)_{12}$ (average 2.877 (3) Å).[9]

All the bridging CO ligands, except CB12–OB12 (which lies on the idealized mirror plane), are more or less asymmetric: those spanning the Rh–Rh edges have longer interactions with Rh3 rather than with the Rh1,2 atoms (average: 2.14 vs 2.05 Å); those spanning the Rh–Os edges have longer interactions with Os rather than with the Rh1,2 atoms (average: 2.20 vs 1.97 Å).

In carbonyl clusters the observed ligand stereochemistry is often the compromise between different requirements; among them the following: (i) the optimization of the interligand interactions; (ii) a good overall charge delocalization; (iii) the fulfillment of local stereochemical needs; (iv) a reasonable local electron bookkeeping on all the metal centers. In order to understand how these factors drive **2** to its unusual geometry, we start from the parent $[Rh_4(CO)_{12}]$ substituting the apical Rh atom with the isoelectronic Os^- fragment,[10] then we bend two equatorial COs to delocalize the charge on the basal triangle, and finally we shorten all the Rh1,2–C_{br} interactions (except those involving CB12) to compensate for the lack of valence electrons on Rh1 and Rh2. Point i, which is often considered the major factor responsible for the ligand stereochemistry, has here little effect; in fact the polyhedron defined by the oxygen atoms (see Figure 3) does not resemble anymore the icosahedron of the parent $[Rh_4(CO)_{12}]$ and clearly shows that CO ligands are grouped around the apical Os atom (which carries five COs), leaving empty volumes below the basal face.

It still remains to explain why the related $[Ir_3M(CO)_{12}]^-$ (M = Fe,[11] Ru[12]) anions, which are also assembled from one d^8 and

(8) (a) Wei, C. H.; Wilkes, G. R.; Dahl, L. F. *J. Am. Chem. Soc.* **1967**, *89*, 4792. (b) Wei, C. H. *Inorg. Chem.* **1969**, *8*, 2384. $[Rh_4(CO)_{12}]$ has idealized C_{3v} symmetry; it consists of a tetrahedral metal cluster where the unique apical Rh atom carries three terminal CO ligands and the basal triangle bears six terminal (three axial and three equatorial) and three double-bridging COs. The polyhedron of oxygen atoms is an approximate icosahedron.

(9) Churchill, M. R.; De Boer, B. G. *Inorg. Chem.* **1977**, *16*, 878.

(10) As a matter of fact the third transition elements prefer the apical position, as far as the $[Rh_4(CO)_{12}]$ stereochemistry is concerned, and this is confirmed for all the mixed-metal clusters so far structurally characterized with such geometry. This is also confirmed for $[Rh_3Ir(CO)_{12}]$, where, nevertheless, there is only IR evidence: Martinengo, S.; Chini, P.; Albano, V. G.; Cariati, F.; Salvatori, T. *J. Organomet. Chem.* **1973**, *59*, 379.

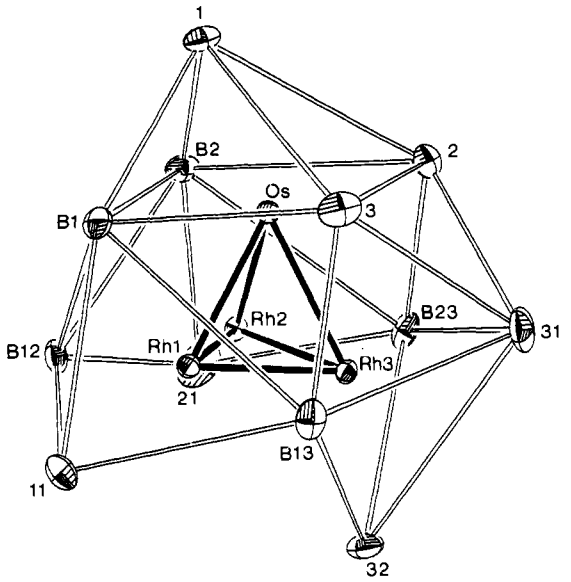

Figure 3. Ligand envelope of $[OsRh_3(CO)_{12}]^-$ obtained by joining the oxygen atoms closer than 5 Å. It does not resemble the icosahedron of the parent $[Rh_4(CO)_{12}]$ and clearly shows that the CO ligands, grouping around the apical Os atom (which carries five COs), leave a hole below the basal face.

Table III. IR Data[a] for $[OsRh_5(CO)_{16}]^-$ and $[OsRh_3(CO)_{12}]^-$

compd	cat. (solv)	CO stretchings
$[OsRh_5(CO)_{16}]^-$	Na^+ (MeOH)	2041 s, 2014 m, 1948 w, 1787 ms
	NEt_4^+ (THF)	2075 w, 2035 s, 2011 m, 1995 sh, 1947 w, 1784 ms
	PPN^+ (THF)	2080 w, 2036 s, 2011 m, 1946 w, 1783 ms
$[OsRh_3(CO)_{12}]^-$	Na^+ (MeOH)[b]	2019 vs, 1990 sh, 1941 mw, 1845 ms
	PPN^+ (THF)	2071 w, 2016 vs, 1993 m, 1938 mw, 1846 ms, 1808 w

[a] Wavenumbers are in cm^{-1} (±3), vs = very strong, s = strong, m = medium, w = weak, and sh = shoulder. [b] Deduced by subtractive IR technique from a mixture.

three d^9 metals, have the $[Rh_4(CO)_{12}]$ stereochemistry and the Fe (or Ru) atoms in the basal triangle. The only remarkable difference concerns the relative kinds of the d^8/d^9 metals: that is, in **2** the d^8 metal belongs to the third transition, while in $[Ir_3M(CO)_{12}]^-$ (M = Fe, Ru) the d^9 metals belong to the third transition. Due to the preference of the third transition elements for the apical position,[10] the Fe^- (or Ru^-) fragment will go into a basal site where, because of the preexisting bridging carbonyls, charge delocalization can occur without any further major stereochemical change, other than the bridge asymmetrization.

4. IR Spectra. Reference IR spectra in THF of (PPN)$[OsRh_5(CO)_{16}]$ and (PPN)$[OsRh_3(CO)_{12}]$ are reported in Figure 4. CO stretchings of derivatives with different cations and in different solvents are reported in Table III. The spectra of both anions show as expected two groups of bands arising in the first case from terminal and triply bridging CO ligands, respectively, and in the latter case to terminal and doubly bridging COs, consistently with the solid-state structures.

5. ^{13}C NMR Spectra. (a) (PPN)$[OsRh_5(CO)_{16}]$. The natural-abundance ^{13}C NMR spectrum of (PPN)$[OsRh_5(CO)_{16}]$, taken at room temperature (297 K) in $CDCl_3$, is consistent with an ideal C_{2v} symmetry of the anion as that reported in Figure 1 with the same atom labeling as previously used,[3,4] in order to facilitate comparison of the data in the Table IV. No fluxionality was observed under these conditions, and this matches the reported

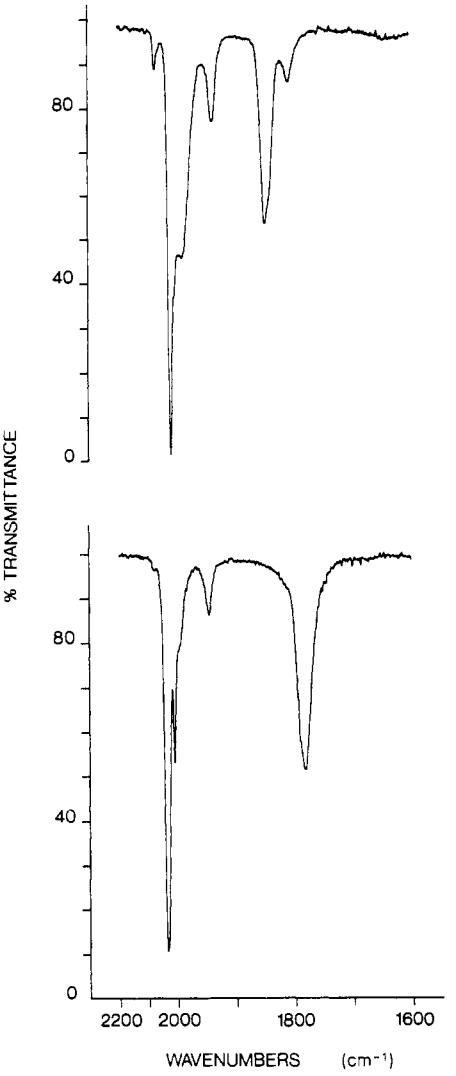

Figure 4. IR spectra in THF of (PPN)$[OsRh_3(CO)_{12}]$ (top) and (PPN)$[OsRh_5(CO)_{16}]$ (bottom).

Table IV. ^{13}C NMR Chemical Shifts of (PPN)$[OsRh_5(CO)_{16}]$ (δ in ppm; J_{Rh-C} in Hz) and Comparison with Those of $[MRh_5(CO)_{16}]^-$ (M = Fe,[3] Ru[4])

	$[OsRh_5(CO)_{16}]^-$	$[RuRh_5(CO)_{16}]^-$	$[FeRh_5(CO)_{16}]^-$
C_a, s	177.71	194.80	211.0
C_b, d	188.21 (67.9)	186.33 (68)	186.8 (70.2)
C_c, d	182.61 (71.4)	184.68 (71)	186.1 (67.1)
C_d, d	184.78 (69.7)	183.82 (70)	184.7 (70.2)
C_e, t	248.67 (ca. 9.5)	255.58 (14.5)	256.8 (12.2)
C_f, q [dt]	239.21 (27.6)	237.83 [30, 25]	233.5 [25.9, 21.4]

behavior of the related isostructural compounds $Rh_6(CO)_{16}$[13] and $[MRh_5(CO)_{16}]^-$ (M = Fe,[3] Ru[4]). There are four distinct sets (a–d) of signals in the terminal CO region (170–190 ppm) and two (e and f) considerably downfield, in the triply bridging CO region. The signal occurring in the terminal region at 177.71 ppm as a singlet of relative intensity 2 is assigned to the Os-bonded carbonyls C_a, while the three doublets must be related to the carbonyls terminally bonded to Rh atoms. The relative intensities of 4, 4, and 2, support the assignment of the latter resonance, at 184.78 ppm (J = 69.7 Hz), to the two carbonyls C_d bonded to the Rh atom trans to the Os in the octahedral cage. The resonances at 182.61 ppm (J = 71.4 Hz) and 188.21 ppm (J = 67.9 Hz) arise from C_b and C_c but, as previously found,[3,4] are not unambiguously assignable.

(11) Della Pergola, R.; Garlaschelli, L.; Demartin, F.; Manassero, M.; Masciocchi, N.; Sansoni, M. *J. Chem. Soc., Dalton Trans.* **1990**, 127.
(12) Fumagalli, A.; Demartin, F.; Sironi, A. *J. Organomet. Chem.* **1985**, *279*, C33.
(13) Heaton, B. T.; Towl, A. D. C.; Chini, P.; Fumagalli, A.; McCaffrey, D. J. A.; Martinengo, S. *J. Chem. Soc., Chem. Commun.* **1975**, 523.

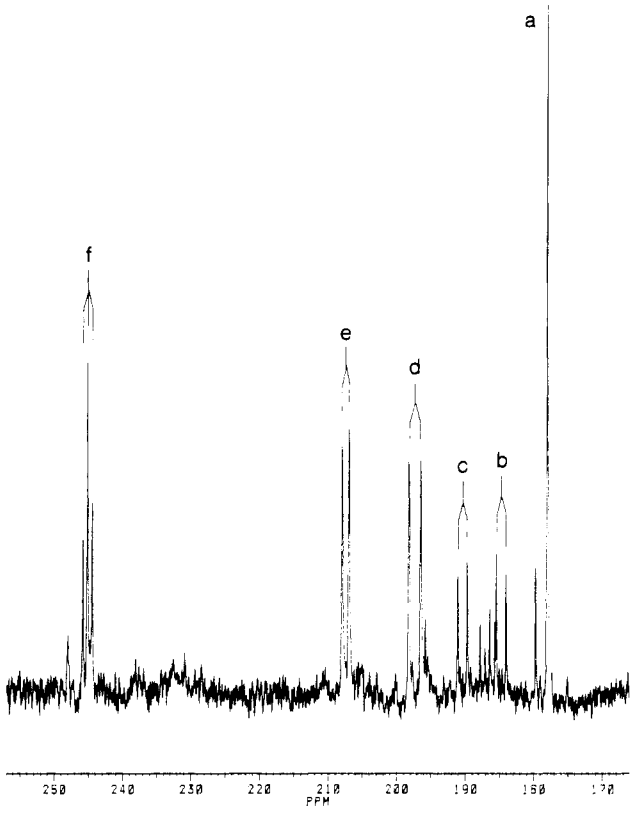

Figure 5. ^{13}C NMR spectrum of $(PPN)[OsRh_3(CO)_{12}]$ in THF-d_8 at 183 K. Resonances b and c are not absolutely assigned and may be interchanged.

The two resonances in the bridging region appear as a triplet, at 248.67 ppm (J ca. 9.5 Hz) and what appears roughly a quartet at 239.21 ppm (J ca. 27 Hz) both with relative intensities of 2; they can be unambiguously assigned respectively to the carbonyls C_e, which bridge $Os-Rh_A-Rh_A$ faces, and C_f, bridging $Rh_A-Rh_A-Rh_B$ faces. This latter signal was expected as a doublet of triplets, and the resemblance to a quartet may arise from similar couplings to Rh_A and Rh_B.

A comparison with the results previously obtained for $[RuRh_5(CO)_{16}]^-$ and $[FeRh_5(CO)_{16}]^-$ (Table IV) indicates remarkable differences for the carbonyls C_a and C_e, which are bonded to the M metal (M = Fe, Ru, Os). The upfield motion of both the signals in the series, on going from Fe to Os, reflects the trend observed in the trinuclear $M_3(CO)_{12}$ series (M = Fe, Ru, Os),[14] which, with average values of 212.9, 199.7, and 176.4 ppm, respectively, are in good agreement with the C_a signals.

(b) $(PPN)[OsRh_3(CO)_{12}]$. The natural-abundance ^{13}C NMR spectrum of $(PPN)[OsRh_3(CO)_{12}]$ in THF-d_6 reported in Figure 5 was taken at the temperature of 183 K, very close to the freezing point of the solution. There are four distinct signals (a–d) in the terminal CO region (170–200 ppm). The three Os-bonded carbonyls give at 177.92 ppm a unique resonance, a singlet of relative intensity 3, which, with reference to Figure 2, is labeled C_a; it must be noted that an analogous steric situation found in $[OsRh_4(CO)_{15}]^{2-}$ gave two distinct signals relative to the single carbonyl trans to an Os–Rh bond and the two which are trans to a bridging CO. The three doublets must be related to the carbonyls terminally bonded to Rh atoms. The two resonances of intensity 1 at 184.69 ppm (J = 71.9 Hz) and 190.35 ppm (J = 68.2 Hz) refer to the two geminal carbonyls bonded to Rh_3, namely C_b, which is almost coplanar to the $Rh_1-Rh_2-Rh_3$ triangle, and C_c, which is trans to Os; they are not unambiguously assignable and could be interchanged. The relative intensity of 2 supports the assignment of the resonance at 197.28 ppm (J = 87.9 Hz) to the two symmetry-related carbonyls C_d bonded to Rh_1 and Rh_2 atoms.

Two signals are in the bridging CO region, a doublet at 207.36 ppm (J = 51.1 Hz) and a remarkably downfield triplet at 245.11 ppm (J = 33.9 Hz) with intensity ratio of 2:3. They can be unambiguously assigned respectively to the two carbonyls C_e, which bridge the $Os-Rh_1$ and $Os-Rh_2$ edges, and to the three carbonyls C_f bridging on the edges of the $Rh_1-Rh_2-Rh_3$ triangle; it is worth noting, with regard to this latter resonance, that consideration of the ideal mirror symmetry of the molecule would lead one to expect two distinct signals in the ratio 1:2.

The other signals appearing in the spectrum are attributable to $[OsRh_5(CO)_{16}]^-$ present as an impurity, which from consideration of the relative intensities may be calculated at a 15–16% level.

At higher temperatures can be observed a fluxionality of the ligands analogous to that of the related $Rh_4(CO)_{12}$.[15] The process is observable as low as 193 K, curiously involving with gradual broadening all the carbonyls except C_b and C_c bonded to Rh_3, which stay sharp; this first part of the process is completed at 233 K when only the two mentioned resonances are recognizable. Upon further temperature increase, at 273 K, carbonyl scrambling is complete and all the signals are lost in the noise; at 323 K they eventually converge in a unique broad signal at 199.87 ppm (weighted mean 204.45 ppm).

Experimental Section

All operations were carried out under N_2 or CO as specified. Tetrahydrofuran was distilled from Na–benzophenone, and 2-propanol was distilled from Al–isopropoxide. All other analytical grade solvents were degassed and stored under N_2. $(PPN)_2[OsRh_4(CO)_{15}]^2$ and $Rh_4(CO)_{12}$[16] were prepared by the published methods, and $Os_3(CO)_{12}$ was obtained commercially. Infrared spectra were recorded on a Perkin-Elmer 781 spectrophotometer equipped with data station for spectral elaboration, using 0.1-mm CaF_2 cells previously purged with nitrogen. ^{13}C NMR spectra were recorded at 50.3 MHz on a Varian instrument, with a resolution of ±1.85 Hz.

1. Synthesis of $[OsRh_5(CO)_{16}]^-$ as the $(NEt_4)^+$ or $(PPN)^+$ Salt. (a) By Reaction of $[OsRh_4(CO)_{15}]^{2-}$ and $[Rh(CO)_2(MeCN)_2]^+$. $(PPN)_2[OsRh_4(CO)_{15}]$ (130.4 mg, 0.062 mmol) and $[Rh(CO)_2(MeCN)_2]BF_4$ (20.4 mg, 0.062 mmol) were placed in a small Schlenk tube under N_2 atmosphere, and THF (3 mL) was added; upon dissolution the color changed readily from yellow to brown. After 2 h of stirring, the solution was cautiously layered with a 1:1 mixture of 2-propanol and hexane (10 mL). When the diffusion was completed (ca. 1 week), after removal of the decanted mother liquor, the black crystals of $(PPN)[OsRh_5(CO)_{16}]$ were washed thoroughly with 2-propanol to remove a little white precipitate which remained suspended (very likely $(PPN)BF_4$) and vacuum dried. Estimated yield: ca. 50 mg.

(b) By Reaction of $[OsRh_4(CO)_{15}]^{2-}$ and $Rh_2(CO)_4Cl_2$. $(PPN)_2[OsRh_4(CO)_{15}]$ (449.7 mg, 0.214 mmol) and $Rh_2(CO)_4Cl_2$ (41.6 mg, 0.107 mmol) were placed in a Schlenk tube under N_2 atmosphere, and THF (10 mL) was added; upon dissolution the color changed readily from yellow to brown. After 15 min of stirring, according to IR monitoring, the equilibrium was reached with only partial formation of $(PPN)[OsRh_5(CO)_{16}]$ and the presence of unreacted $(PPN)_2[OsRh_4(CO)_{15}]$; the situation did not change within the next 24 h. Another portion of $[Rh_2(CO)_4Cl_2]$ (40.0 mg, 0.103 mmol) was added, and within 15 min IR spectroscopy showed complete reaction of the remaining $(PPN)_2[OsRh_4(CO)_{15}]$ with formation essentially of $(PPN)[OsRh_5(CO)_{16}]$; IR subtractive techniques also revealed the presence of $(PPN)[Rh(CO)_2Cl_2]$. The volume of the solution was reduced in vacuum to ca. 3 mL; cautious layering with a 1:1 mixture of 2-propanol and hexane (10 mL) yielded, when the diffusion was completed (ca. 1 week), black crystals of $(PPN)[OsRh_5(CO)_{16}]$ mixed with a tacky material. The mother liquor layered with more hexane (15 mL) yielded a mixture of black and orange crystals, among which were detected $(PPN)[OsRh_5(CO)_{16}]$, $(PPN)[OsRh_3(CO)_{12}]$, and an, as yet, uncharacterized brown species.

(c) By Reduction of $Os_3(CO)_{12}$ and $Rh_4(CO)_{12}$. $Os_3(CO)_{12}$ (119.2 mg, 0.132 mmol) and $Rh_4(CO)_{12}$ (368.2 mg, 0.492 mmol) were placed in a Schlenk tube, which was evacuated and filled with CO and equipped with a small reflux condenser. Methanol (5 mL) and a 2.08 M solution of NaOH in methanol (10 mL) were added, and the mixture was stirred at room temperature for ca. 30 min until the Os carbonyl was dissolved.

(14) Foster, A.; Johnson, B. F. G.; Lewis, J.; Matheson, T. W.; Robinson, B. H.; Jackson, W. G. *J. Chem. Soc., Chem. Commun.* **1974**, 1042.

(15) Cotton, F. A.; Kruczynsky, L.; Shapiro, B. L.; Johnson, L. F. *J. Am. Chem. Soc.* 1972, *94*, 6191.

(16) Martinengo, S.; Giordano, G.; Chini, P. *Inorg. Synth.* **1980**, *20*, 209.

Table V. Crystallographic Data for $(PPN)[OsRh_5(CO)_{16}]$ (I) and $(PPN)[OsRh_3(CO)_{12}]$ (II)

	I	II
formula	$C_{52}H_{30}NO_{16}OsP_2Rh_5$	$C_{48}H_{30}NO_{12}OsP_2Rh_3$
fw	1691.5	1373.6
cryst system	monoclinic	monoclinic
space group	$C2/c$ (No. 15)	$P2_1/c$ (No. 14)
a, Å	33.665 (4)	14.707 (3)
b, Å	9.752 (1)	21.371 (6)
c, Å	33.785 (5)	16.095 (3)
β, deg	94.45 (1)	102.83 (2)
V, Å^3	11058 (4)	4932 (4)
Z	8	4
D_{calc}, g cm^{-3}	2.032	1.850
wavelength, Å	0.710 73	0.710 73
temp, °C	23 ± 2	23 ± 2
linear abs coeff, cm^{-1}	38.52	36.65
R^a	0.030	0.037
R_w^b	0.031	0.037

$^a R = \sum||F_o| - k|F_c||/\sum|F_o|$. $^b R_w = [\sum w(|F_o| - k|F_c|)^2/\sum w|F_o|^2]^{1/2}$.

The resulting green solution was stirred at 60 °C while a slight positive CO pressure was maintained by means of a mercury valve. After about 14 h at this temperature, the green solution with an abundant white precipitate was treated at room temperature with H_3PO_4 (85%, 2 mL); the color changed readily to red-brown. The mixture was again heated at 60 °C under CO for 6–7 h, when the IR spectrum showed essentially the characteristic bands of $Na[OsRh_5(CO)_{16}]$ in methanol at 2040 s, 2014 m, and 1787 mw cm^{-1}. After cooling at room temperature, the white precipitate was filtered off under N_2 atmosphere and washed with 10 mL of methanol, in portions, prior to being discarded. The brown solution, with the collected washings, was treated for metathesis with a solution of $[Et_4N]Br$ (5.1 g in 20 mL of water), giving a brown precipitate which was filtered, thoroughly washed with water (10 mL for 6 times), and vacuum dried for about 1.5 h. Extraction with THF (5 mL) under N_2 gave a solution with a good IR spectrum; slow diffusion of a 1:1 mixture of 2-propanol and hexane (30 mL) cautiously layered on this solution gave, after about 1 week, a brown microcrystalline product. Yield: 250 mg, 50%. Anal. Found: C, 22.35; H, 1.25; N, 1.11. Calcd for $C_{24}H_{20}NO_{16}OsRh_5$: C, 22.47; H, 1.57; N, 1.09. Further addition of 30 mL of hexane to the recrystallization mother liquor gave some more product of lower purity.

The same procedure produced the $(PPN)^+$ salt. The metathesis was done with (PPN)Cl (ca. 2.0 g), and the precipitated salt was recovered as above; recrystallization by the slow diffusion of a 1:1 mixture of 2-propanol and hexane (30 mL) into a THF solution (8–10 mL) gave black crystals. Yield: 360 mg, 53%. Anal. Found: C, 36.63; H, 1.39; N, 0.79. Calcd for $C_{52}H_{30}NO_{16}OsP_2Rh_5$: C, 36.93; H, 1.79; N, 0.83.

2. Synthesis of $(PPN)[OsRh_3(CO)_{12}]$ by Reaction of $(PPN)_2[OsRh_4(CO)_{15}]$ with I_2. A solution of $(PPN)_2[OsRh_4(CO)_{15}]$ (400.2 mg, 0.191 mmol) in 10 mL of THF, under CO, was treated dropwise, while being stirred, with a THF solution of I_2 (0.095 M, 2 mL). After 15 min of stirring, an IR spectrum still showed the presence of traces of $(PPN)_2[OsRh_4(CO)_{15}]$ (very indicative is a band in the bridging region at 1735 cm^{-1}). Further addition of ca. 0.1 mL of I_2 solution completed the reaction, as confirmed by IR spectroscopy after 15 min. The solution was treated with 2-propanol (15 mL) followed by the addition of *n*-hexane (15 mL); this caused selective precipitation of $(PPN)[Rh(CO)_2I_2]$, which was filtered and washed with 10 mL of 2-propanol. The solution and collected washings were concentrated in vacuum to ca. 15 mL to give a yellow-orange precipitate, which, after addition of 15 mL of 2-propanol and 15 min of stirring under N_2, was filtered, washed two times with 5 mL of 2-propanol, and vacuum dried. The product may contain traces of $(PPN)[OsRh_5(CO)_{16}]$ and is recrystallized by dissolution in a mixture of THF and 2-propanol (1:2, v/v; 8 mL); cautious layering of *n*-hexane (20 mL) onto this solution yielded, when the diffusion was completed (ca. 3 days), orange crystals of $(PPN)[OsRh_3(CO)_{12}]$ mixed with a few black crystals of $(PPN)[OsRh_5(CO)_{16}]$. Yield: 190 mg, 72%. Anal. Found: C, 41.49; H, 2.02; N, 0.91. Calcd for $C_{48}H_{30}NO_{12}OsP_2Rh_3$: C, 41.97; H, 2.20; N, 1.02. A ^{13}C NMR spectrum (vide infra) allowed us to set the level of impurity at 15–16%.

3. X-ray Analysis. (a) Collection and Reduction of X-ray Data. A suitable crystal of each compound, $(PPN)[OsRh_5(CO)_{16}]$ (I) and $(PPN)[OsRh_3(CO)_{12}]$ (II), was chosen and each separately mounted on a glass fiber tip onto a goniometer head. Single-crystal X-ray diffraction data were collected on an Enraf-Nonius CAD4 diffractometer with the use of graphite-monochromatized Mo Kα radiation (λ = 0.710 73 Å). The unit cell parameters and an orientation matrix relating the crystal axes to the diffractometer axes were determined by least-squares fit of the setting angles of 25 randomly distributed intense reflections with 10° < θ < 14°. The data collections were performed by the ω-scan method, within the limits 3 < θ < 25° (I) and 3 < θ < 23.5° (II). A total of 9746

Table VI. Selected Fractional Atomic Coordinates and Their Estimated Standard Deviations for $(PPN)[OsRh_5(CO)_{16}]$ (I)

	x	y	z
M1	0.38422 (2)	0.19229 (6)	0.14002 (2)
M2	0.31191 (2)	0.31668 (6)	0.12146 (2)
M3	0.42316 (1)	0.41467 (5)	0.10888 (2)
M4	0.34984 (2)	0.53852 (6)	0.08979 (2)
M5	0.37064 (1)	0.45667 (4)	0.16756 (1)
M6	0.36403 (1)	0.27600 (5)	0.06279 (1)
O11	0.3605 (2)	0.0273 (7)	0.2098 (2)
O12	0.4501 (2)	−0.0040 (6)	0.1220 (2)
O21	0.2715 (2)	0.1753 (7)	0.1869 (2)
O22	0.2357 (2)	0.3670 (8)	0.0713 (2)
O31	0.4947 (2)	0.2678 (7)	0.0821 (2)
O32	0.4710 (2)	0.6701 (6)	0.1286 (2)
O41	0.3861 (2)	0.8196 (6)	0.0903 (3)
O42	0.2814 (2)	0.6255 (8)	0.0319 (2)
O51	0.4030 (2)	0.7348 (6)	0.1948 (2)
O52	0.3432 (2)	0.3710 (7)	0.2469 (2)
O61	0.3010 (2)	0.2933 (9)	−0.0056 (2)
O62	0.4183 (2)	0.0845 (7)	0.0219 (2)
O531	0.4518 (2)	0.3202 (6)	0.1971 (2)
O542	0.2896 (2)	0.6106 (6)	0.1528 (2)
O621	0.3192 (2)	0.0161 (6)	0.0895 (2)
O643	0.4072 (2)	0.5103 (6)	0.0202 (2)
C11	0.3693 (2)	0.0906 (8)	0.1836 (2)
C12	0.4246 (2)	0.0681 (8)	0.1286 (2)
C21	0.2868 (2)	0.2308 (9)	0.1624 (2)
C22	0.2640 (2)	0.3450 (9)	0.0898 (2)
C31	0.4671 (2)	0.3193 (9)	0.0920 (2)
C32	0.4533 (2)	0.5744 (9)	0.1208 (2)
C41	0.3714 (3)	0.7152 (9)	0.0915 (3)
C42	0.3072 (2)	0.5913 (9)	0.0531 (2)
C51	0.3914 (3)	0.6286 (9)	0.1845 (2)
C52	0.3536 (3)	0.4053 (9)	0.2175 (2)
C61	0.3247 (3)	0.285 (1)	0.0199 (2)
C62	0.3977 (2)	0.1544 (9)	0.0373 (2)
C531	0.4253 (2)	0.3403 (9)	0.1739 (2)
C542	0.3147 (2)	0.5371 (9)	0.1436 (2)
C621	0.3339 (2)	0.1202 (8)	0.0964 (2)
C643	0.3953 (2)	0.4661 (9)	0.0487 (2)

Table VII. Selected Fractional Atomic Coordinates and Their Estimated Standard Deviations for $(PPN)[OsRh_3(CO)_{12}]$ (II)

	x	y	z
Os	0.15996 (4)	0.08130 (3)	0.51038 (4)
Rh1	0.34587 (8)	0.10597 (5)	0.48916 (8)
Rh2	0.29972 (8)	0.14652 (5)	0.63551 (8)
Rh3	0.33050 (8)	0.02388 (5)	0.61320 (8)
OB1	0.1973 (7)	0.1479 (5)	0.3467 (7)
O1	−0.0265 (7)	0.1353 (5)	0.4179 (7)
OB2	0.1210 (7)	0.2124 (4)	0.5896 (7)
O2	0.0770 (7)	0.0141 (5)	0.6425 (7)
O3	0.1474 (8)	−0.0368 (5)	0.4022 (8)
O11	0.4795 (8)	0.1377 (6)	0.3782 (8)
OB12	0.3578 (7)	0.2467 (4)	0.5198 (7)
OB13	0.3838 (8)	−0.0333 (4)	0.4539 (7)
O21	0.352 (1)	0.2433 (6)	0.7738 (8)
OB23	0.2777 (8)	0.0619 (5)	0.7822 (6)
O31	0.2565 (9)	−0.1027 (5)	0.6554 (9)
O32	0.5283 (7)	0.0149 (5)	0.7120 (8)
C1	0.0433 (9)	0.1142 (7)	0.451 (1)
CB1	0.2235 (9)	0.1234 (6)	0.414 (1)
C2	0.1100 (9)	0.0391 (7)	0.5942 (9)
CB2	0.1691 (9)	0.1694 (6)	0.586 (1)
C3	0.155 (1)	0.0066 (7)	0.445 (1)
C11	0.427 (1)	0.1263 (7)	0.418 (1)
CB12	0.3433 (9)	0.1964 (6)	0.5386 (9)
CB13	0.3664 (9)	0.0103 (6)	0.491 (1)
C21	0.333 (1)	0.2068 (7)	0.723 (1)
CB23	0.2939 (9)	0.0734 (6)	0.7154 (9)
C31	0.282 (1)	−0.0562 (6)	0.637 (1)
C32	0.454 (1)	0.0189 (7)	0.672 (1)

[5166 with $I > 3\sigma(I)$] (I) and 7919 [3007 with $I > 3\sigma(I)$] (II) diffracted intensities were collected at room temperature with variable scan speed (from 2 to 20° min^{-1}) and a variable scan range of ($\alpha + 0.35 \tan\theta$), with $\alpha = 0.8°$ (I) and $\alpha = 0.9°$ (II); the maximum scanning time for reflections was 60 (I) and 70 s (II). The crystal stability under diffraction condition was checked by monitoring three standard reflections every 60 min, and no crystal decay was observed. The measured intensities were corrected for Lorentz, polarization, and background effects and reduced to F_o. An empirical absorption correction was applied as described[17] using ψ-scans of three suitable reflections having χ values close to 90°.

(b) Solution and Structure Refinement. Crystal data are summarized in Table V. For compound I the metal atoms positions were taken from that of the isomorphous $(PPN)[RuRh_5(CO)_{16}]$[4] in the centrosymmetric space group $C2/c$ (No. 15). For compound II from systematic absences ($0k0$, $k = 2n + 1$; $h0l$, $l = 2n + 1$), the centrosymmetric space group $P2_1/c$ (No. 14) was uniquely determined. The positions of the four metal atoms were obtained from a Patterson map. In both structures the remaining lighter P, O, N, and C atoms were located from subsequent difference Fourier syntheses; the hydrogen atoms of the PPN cations were placed in idealized positions (C-H = 0.95 Å) and refined riding on their parent atoms with fixed isotropic thermal parameters ($B = 5.0$ Å^2). Anisotropic thermal parameters were assigned to all the atoms of the anions and to the P atoms of the cations, while to the N and C atoms of the cations were given isotropic B's. Full-matrix least-squares refinement of 515 (I) and 419 (II) variables converged to R, R_w, and GOF factors of 0.030, 0.031, and 1.166 (I) and 0.037, 0.037, and 1.138 (II), the minimized function being $\sum w(|F_o| - k|F_c|)^2$. Individual weights were assigned as $w = 1/\sigma^2(F_o)$, where $\sigma(F_o) = \sigma(F_o^2)/2F_o$ and $\sigma(F_o^2) = [\sigma^2(I) + (pI)^2]^{1/2}/LP$, where $\sigma(F_o^2)$ is the standard deviation for each reflection as derived from counting statistics, p (0.030 for I and 0.035 for II is a coefficient for improving the goodness of fit, and LP is the Lorentz-polarization factor. In compound I all the metal atoms were found having variable mixed Os/Rh occupancies; practically, we refined all the metals as Rh atoms with free multiplicities. This lead to the final values of 1.04, 1.04, 1.12, 1.05, 1.31, and 1.13 for the M1-M6 multiplicities, respectively, in perfect agreement with the presence of just one Os atom. In the last residual Fourier map, peaks not exceeding 0.43 (I) and 0.56 (II) e/Å^3 were found. Scattering factors for neutral atoms and anomalous dispersion corrections for scattering factors were taken from refs 18 and 19, respectively. Final selected atomic coordinates with their estimated standard deviations are presented in Tables VI (I) and VII (II), respectively. All the calculations were performed on a PDP 11/73 computer using the SDP-Plus structure determination package.[20]

Supplementary Material Available: Detailed lists of crystallographic parameters (Tables S1 (I) and S7 (II)), full lists of atomic coordinates (Tables S2 (I) and S8 (II)), lists of anisotropic thermal factors (Tables S3 (I) and S9 (II)), and full lists of bond distances and angles (Tables S4 and S5 (I) and Tables S10 and S11 (II)) (18 pages); lists of observed and calculated structure factor moduli (Tables S6 (I) and S12 (II)) (56 pages). Ordering information is given on any current masthead page.

(17) North, A. C. T.; Phillips, D. C.; Mathews, F. S. *Acta Crystallogr., Sect. A* **1968**, *24*, 351.
(18) Cromer, D. T. *International Tables for X-Ray Crystallography*; The Kynoch Press: Birmingham, England, 1974 (present distributor Kluwer Academic Publishers, Dordrecht, The Netherlands); Vol. 4, Table 2.3.1.
(19) Cromer, D. T.; Waber, J. T. *International Tables for X-Ray Crystallography*; The Kynoch Press: Birmingham, England, 1974 (present distributor Kluwer Academic Publishers, Dordrecht, The Netherlands); Vol. 4, Table 2.2.b.
(20) Frenz, B. A.; et al. *SDP Structure Determination Package Plus*, Version 1.0; Enraf-Nonius: Delft, The Netherlands, 1980.

Contribution from the Departments of Chemistry, University of Warwick, Coventry, U.K., and Imperial College of Science, Technology and Medicine, London, U.K.

Ruthenatetraboranes: Synthesis of $[Ru(B_3H_8)(PPh_3)\{HB(pz)_3\}]$ and Crystal Structure of $[RuCl(PPh_3)_2\{HB(pz)_3\}]$ (pz = Pyrazol-1-yl)

Nathaniel W. Alcock,[†] Ian. D. Burns,[‡] Kanwaljit S. Claire,[†] and Anthony F. Hill*[,‡]

Received December 20, 1991

The reaction of $[RuCl_2(PPh_3)_3]$ with $K[HB(pz)_3]$ (pz = pyrazol-1-yl) affords $[RuCl(PPh_3)_2\{\kappa^3\text{-}HB(pz)_3\}]$ [crystallographically characterized with monoclinic crystals of space group $P2_1/a$, $Z = 8$, in a unit cell of dimensions $a = 19.75$ (1) Å, $b = 22.48$ (1) Å, $c = 20.283$ (7) Å, and $\beta = 112.94$ (3)°], which upon treatment with $NR_4[B_3H_8]$ (R = Me, Bu) provides the ruthenatetraborane $[Ru(B_3H_8)(PPh_3)\{\kappa^3\text{-}HB(pz)_3\}]$.

Introduction

Metallaboranes of low nuclearity, in particular the metallatetraboranes, are of interest as possible precursors to clusters of higher nuclearity.[1] Nevertheless very little is known about the reactivity of these compounds. The established reactions of metal octahydrotriborates are essentially limited to (i) displacement of the B_3H_8 moiety,[2] (ii) halogenation of the unique wingtip BH_2 group,[3] (iii) *agostic* coordination of the wingtip BH_2 group to an otherwise coordinatively unsaturated metal center,[3] and (iv) dehydrohalogenative formation of boraallyl complexes[4,5] (by implication). We describe here the convenient synthesis of an air-stable ruthenatetraborane from the new complex $[RuCl(PPh_3)_2\{\kappa^3\text{-}HB(pz)_3\}]$ (pz = pyrazol-1-yl).

Results and Discussion

Synthesis of $[RuCl(PPh_3)_2\{\kappa^3\text{-}HB(pz)_3\}]$. The complex $[RuCl_2(PPh_3)_3]$[6] has been shown to react with TlC_5H_5 to provide the half-sandwich compound $[RuCl(PPh_3)_2(\eta^5\text{-}C_5H_5)]$,[7] the chemistry of which is sufficiently rich to deserve review in its own right.[8] The firmly established analogy between the ligands η-C_5H_5 and κ^3-$HB(pz)_3$ suggests that a similarly rich chemistry should be anticipated for the complex $[RuCl(PPh_3)_2\{\kappa^3\text{-}HB(pz)_3\}]$. We have obtained this compound by the simple reaction of Wilkinson's

Scheme I

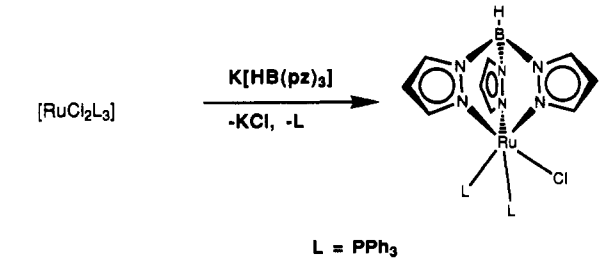

L = PPh_3

† University of Warwick.
‡ Imperial College.

(1) Kennedy, J. D. *Prog. Inorg. Chem.* **1984**, *32*, 519.
(2) Klanberg, F.; Muetterties, E. L. *J. Am. Chem. Soc.* **1968**, *90*, 3296.
(3) Gaines, D. F.; Hildebrandt, S. J. *Inorg. Chem.* **1978**, *17*, 794.
(4) Guggenberger, L. J.; Kane, A. R.; Meutterties, E. L. *J. Am. Chem. Soc.* **1972**, *94*, 5665.
(5) Greenwood, N. N.; Kennedy, J. D.; Reed, D. *J. Chem. Soc., Dalton Trans.* **1980**, 196. Bould, J.; Greenwood, N. N.; Kennedy, J. D.; McDonald, W. S. *J. Chem. Soc., Dalton Trans.* **1985**, 1843.
(6) Hallman, P. S.; Stephenson, T. A.; Wilkinson, G. *Inorg. Synth.* **1970**, *12*, 237.
(7) Blackmore, T.; Bruce, M. I.; Stone, F. G. A. *J. Chem. Soc. A* **1971**, 2376.

0020-1669/92/1331-2906$03.00/0